





Supplementary Power Control of an HVDC System and Its Impact on Electromechanical Dynamics

Danilo Obradović , *Student Member, IEEE*, Marina Oluić , *Member, IEEE*,
Robert Eriksson , *Senior Member, IEEE*, and Mehrdad Ghandhari , *Senior Member, IEEE*

Abstract—This paper presents a comprehensive analysis of the impact that supplementary power control of an HVDC link has on the electromechanical dynamics of power systems. The presented work addresses an interesting phenomenon that may occur when an HVDC power controller is installed to support frequency stability. In specific cases, a high gain HVDC frequency controller could deteriorate system damping. The given analytical study is the first of its kind that addresses this issue by including both: (i) the important higher-order generator dynamics that affect small signal stability simultaneously with an HVDC control as well as (ii) the available local angle/frequency input signals of the controller. The methodological approach here analytically formulates the impact an HVDC control has on the single generator dynamics. Furthermore, the relationship between the damping/synchronizing coefficients and the HVDC gain is explicitly derived when a frequency proportional HVDC controller is installed. The derived expressions confirm that, indeed, there is an optimal HVDC gain with respect to the damping coefficient and a typically positive impact of the HVDC controller on the synchronizing component. Finally, the developed theoretical foundation is demonstrated by the tools of linear and nonlinear analysis in a one-machine system case study.

Index Terms—Active power control, frequency stability support, high voltage direct current (HVDC) system, power system dynamics, small signal stability assessment.

I. INTRODUCTION

ENSURING a high share of renewable energy sources is an important step towards more sustainable power systems [1]. Yet, integration of renewables introduces a number of technical challenges, including those related to system stability [2]–[5]. Particularly prone are the events on the electromechanical timescale due to a direct influence of renewables on the frequency stability. Owing to the development of new types of frequency support controllers (e.g. High Voltage Direct Current (HVDC)-based solutions), integration of renewables indirectly also affects other dynamical aspects in the power system, such

as transient and Small Signal Stability (SSS). Therefore, it is important to investigate both: (i) the relationship between the design of contemporary frequency controls and system response to disturbed conditions and (ii) possible side-effects of such a set-up in the framework of electromechanical dynamics.

Given the nowadays circumstances, the presented stability issues impose a need for an efficient coordination between the control elements of power systems. Due to their high speed of response and flexibility in control design, the “asynchronous” HVDC interconnections are widely-perceived as a potential remedy to some of the aforementioned stability challenges [6]–[9]. Although HVDC systems offer a broad spectrum of control modes, the high uncertainty in system operation makes the simple and robust solutions more attractive. For the purpose of supporting frequency stability, a simple control of the HVDC active power injection proportional to frequency deviation is often considered as a safe choice [10]. Many existing works have noticed that this “classical approach” also improves the SSS. This correlation was systematically discussed when generators were represented by the classical model and local input signal was approximated as a linear combination of remote ones (generator speeds) [11], [12].

Some case studies have, however, detected situations for which the frequency support provided by an HVDC system adversely affects the SSS margin [13], [14]. These findings are in line with the conclusions of related research branches that aimed to damp the electromechanical oscillations through the power modulation (of e.g. loads or wind power plants) [15]–[19]. The earlier such analyses reported that a proportional active power control with a local frequency deviation input may deteriorate SSS and induce electromechanical oscillations if the controller gain becomes too high [15]–[17]. Namely, a gain too high can cause the root locus of the corresponding critical electromechanical mode to move toward the respective open loop zero that could be less damped. Besides, more recent studies have demonstrated that even with the optimal choice of control input signal (phase angle) [18], the non-existence of zeros in the right hand side of the complex plane cannot be assured in general control configuration [19].

In summary, an overall positive impact of the aforementioned supplementary HVDC control on SSS is observed in the literature. Still, there have been cases where the damping reduction of the electromechanical modes is noticed, but not fully assessed [13], [14]. Another flaw of the similar existing studies is neglectation of higher order generator dynamics.

Manuscript received August 13, 2020; revised December 15, 2020; accepted January 24, 2021. Date of publication February 4, 2021; date of current version August 19, 2021. This work was supported in part by the MultiDC project, in part by Innovation Fund Denmark, under Grant Agreement 6154-00020B. Paper no. TPWRS-01376-2020. (*Corresponding author: Danilo Obradović.*)

Danilo Obradović, Marina Oluić, and Mehrdad Ghandhari are with the KTH Royal Institute of Technology, 100 44 Stockholm, Sweden (e-mail: daniloo@kth.se; oluic@kth.se; mehrdad@kth.se).

Robert Eriksson is with the Department of System Development, Svenska kraftnät, 172 24 Sundbyberg, Sweden (e-mail: robert.eriksson@svk.se).

Color versions of one or more figures in this article are available at <https://doi.org/10.1109/TPWRS.2021.3056763>.

Digital Object Identifier 10.1109/TPWRS.2021.3056763

Furthermore, due to their challenging analytical incorporation, the local input (frequency or phase angle) measurements have previously been approximated in the analysis by a combination of remote signals that cannot be measured in reality without additional infrastructure [11], [12].

The contributions of this paper (C1-C4) and their significance for the topic of interest are provided in the following.

C1: Firstly, the work asserts the existing drawbacks by providing the analytical formulation of the impact that an HVDC supplementary power control has on electromechanical dynamics by employing a generic, one-machine infinite-bus system. To the best of authors' knowledge, this is the first analytical study of the sort that accounts for more detailed generator modeling—the dynamics of both Automatic Voltage Regulator (AVR) and Power System Stabilizer (PSS) are included. In the previous literature, the analytical studies have only considered the classical model for the generators. The specific derivations presented in this paper (which retained the control structure of the Heffron-Phillips model [4]) enabled the adaptation of the AVR and PSS transfer functions in order to integrate the HVDC contribution.

C2: Moreover, this is all carried out by incorporating an input signal (phase angle) that is available from the existing infrastructure of an HVDC system.

C3: As a result, the influence of HVDC control over electromechanical mode was formalized by finding the explicit expressions for changes in synchronizing and damping torque coefficients as functions of the HVDC proportional controller gain. Such analytical relationships were not discussed before for this type of controller in the existing literature, particularly in the connection to the system's properties such as configuration, operating point and controller gains. Hence, although the SSS analysis is a classical, well-known tool for the study of electromechanical dynamics, its properties have not been utilized for this specific purpose in the past.

C4: Finally, the paper carries out a structured analysis of the obtained expressions with respect to the value of the HVDC gain. The key goal is to understand and explain for which cases positive or negative effects of the HVDC control are present. Such analysis is significant since it simultaneously considers the overlapping mechanisms originating from other important SSS contributors (AVR and PSS). In the study, the existence of an optimal HVDC gain of the supplementary power control with respect to the maximum damping torque coefficient is confirmed and derived. After this value of the gain, the damping torque coefficient starts decreasing. It is to be pointed out that the performed analysis is further applicable to other controller types that use local measurements of phase angle/frequency as the control inputs.

The rest of the paper is organized as follows. Section II presents the linearized dynamics of the generic system (including HVDC control) and the theoretical basin for further derivations. In Section III, the explicit expressions for the changes in damping and synchronizing torque coefficients are provided when supplementary HVDC control proportional to frequency is being taken into account. Section IV carries out a detailed analysis of the obtained expressions and tests the analytically

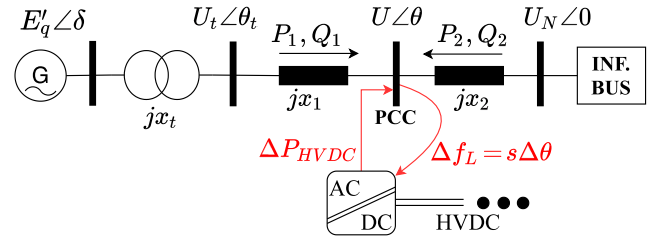


Fig. 1. SMIB system with HVDC supplementary power control.

derived concepts by employing one-machine system in the case study. Finally, general conclusions and remarks are summarized in Section V.

II. SUPPLEMENTARY POWER CONTROL OF AN HVDC LINK IN A SINGLE-MACHINE INFINITE-BUS SYSTEM

To guarantee a safe operation of a power system with respect to comparatively smaller disturbances, the system needs to be small signal stable at all times. The task of Small Signal Stability (SSS) analysis is to maintain the pre-defined stability margins of the system while ensuring the quality of both power and frequency. The fulfillment of this task reflects through a sufficient synchronizing and damping component of critical (inter/intra-area) electromechanical modes that originate from electromechanical oscillations which are inherent to synchronous generators. A violation of SSS requirements could result in undesirable system separation that may occur even as a consequence of normal fluctuations in the quasi-steady-state [4]. Now, since HVDC frequency support controls can interfere with SSS, it is important to examine their exact effect to make sure that the improvement of one category of stability (e.g. frequency) does not harm other stability types.

For this purpose, the following section constructs a theoretical foundation for the SSS assessment of a system shown in Fig. 1, which actually represents a Single-Machine Infinite-Bus (SMIB) system with addition of an HVDC supplementary power controller. The aim is to derive an explicit relationship that describes how a supplementary HVDC power control affects linearized generator dynamics. The generator is here represented by the one-axis model [4] and has both an AVR and a PSS installed.

The motivation for using such a simple set-up arises from the possibility to clearly outline the effect of the supplementary HVDC power control on SSS. Typically, the non-linear dynamics of a general power system are described by a set of Differential-Algebraic Equations (DAE):

$$\begin{aligned} \dot{\mathbf{x}} &= \mathbf{f}(\mathbf{x}, \mathbf{y}); \\ \mathbf{0} &= \mathbf{g}(\mathbf{x}, \mathbf{y}), \end{aligned} \quad (1)$$

where \mathbf{x} and \mathbf{y} are the vectors of state and algebraic variables, respectively. When applied to the system in Fig. 1 without HVDC control taken into account, the differential equations $\mathbf{f}(\mathbf{x}, \mathbf{y})$ obtain the following form:

$$\begin{aligned}
 \dot{\delta} &= \omega; \\
 \dot{\omega} &= \frac{1}{M} (P_m - P_e) = \frac{1}{M} \left(P_m - \frac{E'_q U}{x'_d + x_1} \sin(\delta - \theta) \right); \\
 \dot{E}'_q &= \frac{1}{T'_{do}} \left(E_f - \frac{x_d + x_1}{x'_d + x_1} E'_q + \frac{x_d - x'_d}{x'_d + x_1} U \cos(\delta - \theta) \right); \\
 \dot{E}_f &= \frac{1}{T_e} \left(-E_f + K_A \left(U_{ref} - U_t + \frac{T_1}{T_2} \left(\frac{K_{pss}}{\omega_n} \omega - S_1 \right) + S_2 \right) \right); \\
 \dot{S}_1 &= \frac{1}{T_W} \left(\frac{K_{pss}}{\omega_n} \omega - S_1 \right); \\
 \dot{S}_2 &= \frac{1}{T_2} \left(\left(1 - \frac{T_1}{T_2} \right) \left(\frac{K_{pss}}{\omega_n} \omega - S_1 \right) - S_2 \right), \quad (2)
 \end{aligned}$$

where the d -axis reactances (x_d and x'_d) include the reactance of the transformer x_t and all other variables and parameters comply with the standardized notation from [4], [20]. The AVR (for which the terminal voltage is used as the input) is of static type and the PSS dynamics are given for one lead-lag filter ($n_f = 1$). Still, the analysis is also applicable to higher orders of PSS dynamics. Algebraic equations $g(x, y)$ describe active and reactive power balances in the system. For the Point of Common Coupling (PCC) in Fig. 1 where an HVDC system/link is planned to be connected, the power balance equations can be written as:

$$0 = P_1 + P_2; \quad (3a)$$

$$0 = Q_1 + Q_2, \quad (3b)$$

for the case without an HVDC system. The powers P_1 , P_2 , Q_1 and Q_2 are given in (45a)–(45b) of Appendix VII. Linearization of the DAE model from (2)–(3b) is a reliable (and standard) tool for assessment of the system dynamics. Once the linearization is carried out, the idea is to include the HVDC supplementary power control into the Heffron-Phillips model [21] in such a way that the system structure remains the same. In this manner, after obtaining the compact form of the modified Heffron-Phillips model (by applying the Mason's rule [22]), the properties of that model can be used directly.

As shown in further derivations from Section III, the perturbation in generator active power ΔP_e can be expressed in the terms of the synchronizing and damping components, which are in phase with the change of the generator rotor angle $\Delta\delta$ and angle speed $\Delta\omega$, respectively. To formalize this concept, the synchronizing coefficient (K_S) and the damping coefficient (K_D) of the interesting electromechanical mode $\bar{\lambda}_p$ were introduced in the literature. These coefficients are widely-recognized as a measure of both SSS and transient stability of a power system [4], [20]. If the values of the two coefficients become larger, the stability margin will increase, as well. The relationship between the change in generator active power and these coefficients (in general) is the following:

$$\Delta P_e|_{(s=\bar{\lambda}_p)} = K_S \Delta\delta + K_D \Delta\omega, \quad (4)$$

where s is a Laplace operator, and for the purpose of obtaining K_S and K_D it is set to be equal to the mode of interest $\bar{\lambda}_p$. The

goal here is to describe how a supplementary control of HVDC system active power will contribute to the synchronizing and damping torque coefficients that relate to generator electromechanical modes of interest. To identify the impact of the HVDC controller on K_S and K_D parameters analytically, the power balance from (3a) is first extended for the active power of the HVDC system (P_{HVDC}) and then linearized as:

$$\Delta P_1 + \Delta P_2 + \Delta P_{HVDC} = 0, \quad (5)$$

where the changes in active power contributions of the generator and infinite bus are given with:

$$\Delta P_e = l_1 (\Delta\delta - \Delta\theta) + \frac{P_{e0}}{E'_{q0}} \Delta E'_q + \frac{P_{e0}}{U_0} \Delta U;$$

$$\Delta P_2 = -l_2 \Delta\theta - \frac{P_{e0}}{U_0} \Delta U, \quad (6)$$

respectively, while l_1 and l_2 are defined in (47) of Appendix A. In all the power contributions, the variables containing subscript “0” refer to the initial operating point and the ones with “ Δ ” represent a general, small deviation from this operating point (around which the linearization has been carried out). What remains here is to linearize the HVDC system-related part of (5) by taking into account the contribution of the HVDC control. In that sense, let the HVDC control be given by:

$$\Delta P_{HVDC} = F'(s) \Delta f_L = F'(s) s \Delta\theta = F(s) \Delta\theta, \quad (7)$$

where $F(s)$ represents the function of the supplementary HVDC power controller, and Δf_L is the local frequency deviation. When it comes to the frequency control of large-scale power systems, a local information is typically preferred in practice since it does not impose the requirement to build additional communication infrastructure.

This paper has now incorporated the effects of the HVDC control that uses local input signal (frequency or phase angle deviation), too. As a result, no remote information need to be used as the input to the HVDC controller and the HVDC control function $F(s)$ can be arbitrarily chosen. Finally, the replacement of (6)–(7) into (5) with $l_{12} = l_1 + l_2$ yields the relationship between the change in $\Delta\theta$ and the state variables ($\Delta\delta$, $\Delta E'_q$):

$$\Delta\theta = \frac{1}{l_{12} - F(s)} \left(l_1 \Delta\delta + \frac{P_{e0}}{E'_{q0}} \Delta E'_q \right). \quad (8)$$

In a similar manner, by linearizing (3b) (and by assuming that Q_{HVDC} is perfectly controlled to be zero):

$$\Delta Q_1 + \Delta Q_2 = 0, \quad (9)$$

the respective reactive powers become as follows:

$$\begin{aligned}
 \Delta Q_1 &= \frac{U_0}{x_1 + x'_d} \Delta U + \frac{Q_{10}}{U_0} \Delta U + P_{e0} (\Delta\delta - \Delta\theta) - \frac{l_1}{E'_{q0}} \Delta E'_q; \\
 \Delta Q_2 &= \frac{U_0}{x_2} \Delta U - \frac{Q_{10}}{U_0} \Delta U + P_{e0} \Delta\theta.
 \end{aligned} \quad (10)$$

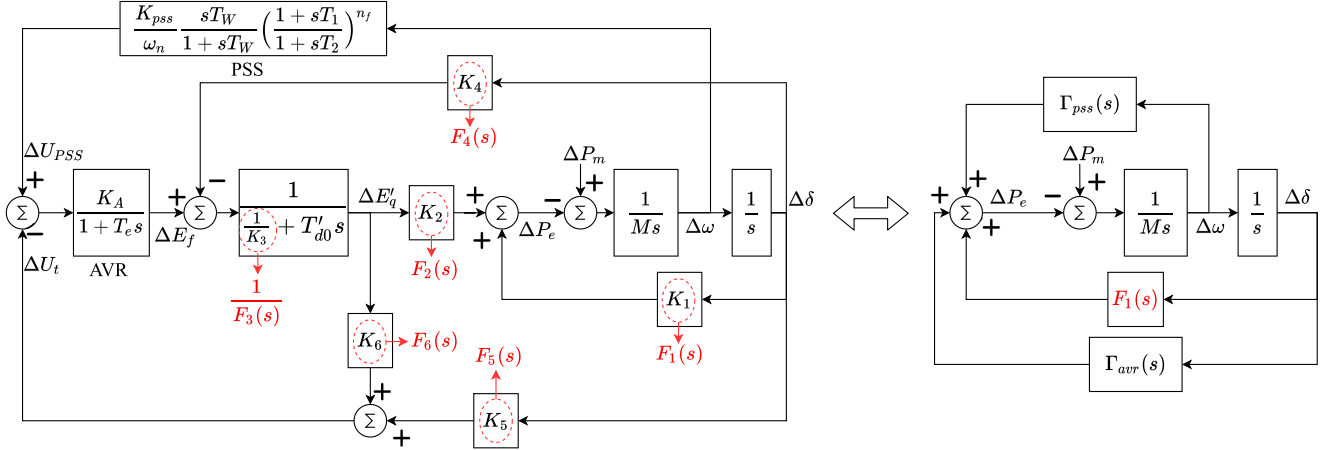


Fig. 2. Heffron-Phillips model without and with HVDC supplementary control: with HVDC control, the contribution constants K_i become Laplace functions $F_i(s)$: $K_i \Rightarrow F_i(s)$ ($i = 1, \dots, 6$); the compact representation is given on the right side.

Then, a direct relationship between ΔU and the state variables ($\Delta\delta$, $\Delta E'_q$) can be obtained as:

$$\Delta U = \frac{U_0}{l_{12}} \left(-P_{e0} \Delta\delta + \frac{l_1}{E'_{q0}} \Delta E'_q \right). \quad (11)$$

From (8) and (11), the change in generator active power can be expressed only in the terms of generator state variables and the contribution of the supplementary HVDC control:

$$\begin{aligned} \Delta P_e &= \left(l_1 \frac{l_2 - F(s)}{l_{12} - F(s)} - \frac{P_{e0}^2}{l_{12}} \right) \Delta\delta \\ &+ \frac{P_{e0}}{E'_{q0}} \left(1 + \frac{l_1}{l_{12}} - \frac{l_1}{l_{12} - F(s)} \right) \Delta E'_q \\ &= F_1(s) \Delta\delta + F_2(s) \Delta E'_q, \end{aligned} \quad (12)$$

where $F_1(s)$ and $F_2(s)$ are the functions that include the HVDC control. The goal here is to find the expression for the change in active generator power that has the form of (4). For this purpose, $\Delta E'_q$ first needs to be given via $\Delta\delta$ and $\Delta\omega$.

This task will be addressed similarly as in [21] by establishing the following relationship:

$$F_2(s) \Delta E'_q = \Gamma_{avr}(s) \Delta\delta + \Gamma_{pss}(s) \Delta\omega, \quad (13)$$

while retaining the control structure of the classical Heffron-Phillips model [21] with the addition of the HVDC control, as illustrated in Fig. 2. Then, by applying Mason's rule (similarly as in [21]), the transfer functions that describe AVR and PSS dynamics in (13) are defined as:

$$\begin{aligned} \Gamma_{avr}(s) &= \frac{-F_2(s) [K_A F_5(s) + F_4(s) + s T_e F_4(s)]}{\frac{1}{F_3(s)} + K_A F_6(s) + s \left(\frac{T_e}{F_3(s)} + T'_{do} \right) + s^2 (T'_{do} T_e)}; \\ \Gamma_{pss}(s) &= \frac{G_{pss}(s) F_2(s) K_A}{K_A F_6(s) + \left(\frac{1}{F_3(s)} + s T'_{do} \right) (1 + s T_e)}, \end{aligned} \quad (14)$$

where $G_{pss}(s)$ represents a PSS transfer function between input $\Delta\omega$ and output ΔU_{PSS} , as shown in Fig. 2. The transfer functions introduced here by (14) are constructed such that they take into account the HVDC control while also working for the case without an HVDC control contribution ($F(s) = 0$) for which $F_i(s) = K_i$ ($i = 1, \dots, 6$). This property is enabled by simply defining:

$$\begin{aligned} F_i(s) &= K_i + \Delta F_i(s), \text{ for } i = 1, \dots, 6 \wedge i \neq 3 \text{ and} \\ \frac{1}{F_i(s)} &= \frac{1}{K_i} + \Delta F_i(s), \text{ for } i = 3, \end{aligned} \quad (15)$$

where the functions $F_i(s)$ and HVDC control contributions $\Delta F_i(s)$ are derived and presented in (48)–(53) of Appendix A. Finally, by the virtue of derived functions ($F_i(s)$) and (12)–(13), the generator active power can be expressed as:

$$\Delta P_e = (\Gamma_{avr}(s) + F_1(s)) \Delta\delta + \Gamma_{pss}(s) \Delta\omega. \quad (16)$$

At this point, all the algebraic variables have been eliminated and the contribution of HVDC supplementary control to generator dynamics has received its analytical formulation. The presented generic approach provides a possibility to observe and analyze the interaction between the HVDC control and generator dynamics with AVR and PSS included. The properties of the derived AVR/PSS transfer functions from (14) at electromechanical modes will be used for the further analysis in the upcoming section.

III. ANALYTICAL DERIVATION OF CHANGES IN K_S AND K_D WITH SUPPLEMENTARY HVDC POWER CONTROL

Once that the exact analytical relationship “generator power-HVDC supplementary control” is established in Section II, some convenient SSS properties will be exploited to simplify (16). It is first of interest to make this relationship more direct with respect to the specific case of electromechanical modes that are of importance for SSS analysis. The frequencies of electromechanical modes are ranging up to about 3 Hz. The adoption of typical generator parameter values and methods for

tuning AVR/PSS allows the functions $\Gamma_{avr}(s)$ and $\Gamma_{pss}(s)$ to be represented similarly as in [21]:

$$\Gamma_{avr}(s) = \frac{-F_2(s)F_5(s)}{K_6 \left(1 + s \frac{T'_{d0}}{K_A K_6}\right) (1 + sT_e)};$$

$$\Gamma_{pss}(s) = \frac{F_2(s)}{K_6} \frac{G_{pss}(s)}{\left(1 + s \frac{T'_{d0}}{K_A K_6}\right) (1 + sT_e)}, \quad (17)$$

for the aforementioned modes. Equations (17) imply that only $F_2(s)$ and $F_5(s)$ functions affect $\Gamma_{avr}(s)$ and $\Gamma_{pss}(s)$.

Now, let all the functions and parameters related to the case without an HVDC control contribution ($F_i(s) = K_i$, $i = 1, \dots, 6$) be marked with tilde sign. Then, for the mode of interest, (16) becomes:

$$\begin{aligned} \Delta \tilde{P}_e|_{(s=\tilde{\lambda}_p)} &= (\tilde{\Gamma}_{avr}(s) + K_1)\Delta\delta + \tilde{\Gamma}_{pss}(s)\Delta\omega \\ &= \tilde{K}_S\Delta\delta + \tilde{K}_D\Delta\omega, \end{aligned} \quad (18)$$

and the relationship between $\Gamma/\tilde{\Gamma}$ functions from the two cases (with/without HVDC system) is straightforward to be derived:

$$\begin{aligned} \Gamma_{avr}(s) &= \tilde{\Gamma}_{avr}(s) \left(1 + \frac{\Delta F_2(s)}{K_2} + \frac{\Delta F_5(s)}{K_5}\right); \\ \Gamma_{pss}(s) &= \tilde{\Gamma}_{pss}(s) \left(1 + \frac{\Delta F_2(s)}{K_2}\right). \end{aligned} \quad (19)$$

Now, with the inclusion of the HVDC control (and $s = \tilde{\lambda}_p + \Delta\tilde{\lambda}_p$), (18) can be rewritten as:

$$\Delta P_e = (\tilde{K}_S\Delta\delta + \tilde{K}_D\Delta\omega) + \Delta K_S\Delta\delta + \Delta K_D\Delta\omega, \quad (20)$$

where $\Delta K_S/\Delta K_D$ and $\Delta\tilde{\lambda}_p$ represent the changes of synchronizing/damping coefficients an the mode of interest due to HVDC control, respectively. Furthermore, by using the expressions from (53), the replacement of (19) into (16) results in:

$$\begin{aligned} \Delta P_e &= \left((\tilde{\Gamma}_{avr}(s) + K_1)\Delta\delta + \tilde{\Gamma}_{pss}(s)\Delta\omega \right) \left(1 + \frac{\Delta F_2(s)}{K_2} \right) \\ &+ \left(\frac{l_{12}}{l_{1d} + l_2} \tilde{\Gamma}_{avr}(s) + \frac{\Delta F_1(s)K_2}{\Delta F_2(s)} - K_1 \right) \frac{\Delta F_2(s)}{K_2} \Delta\delta, \end{aligned} \quad (21)$$

as shown in (54) of the Appendix B.

Previously, in [20], [23], it was observed that a high AVR gain implies a constant contribution to the synchronizing torque coefficients and that the PSS provides a constant damping for small variations of the electromechanical modes (without an HVDC system). With respect to this, let:

$$\begin{aligned} \tilde{\Gamma}_{avr}|_{(s=\tilde{\lambda}_p+\Delta\tilde{\lambda}_p)} &\approx \tilde{\Gamma}_{avr}|_{(s=\tilde{\lambda}_p)} = \text{const.} \in \mathbb{C}; \\ \tilde{\Gamma}_{pss}|_{(s=\tilde{\lambda}_p+\Delta\tilde{\lambda}_p)} &\approx \tilde{\Gamma}_{pss}|_{(s=\tilde{\lambda}_p)} = \text{const.} \in \mathbb{C}, \end{aligned} \quad (22)$$

be assumed to hold for $\tilde{\lambda}_p + \Delta\tilde{\lambda}_p$ that is located in the proximity to the initial $\tilde{\lambda}_p$. By using this property, (21) can be reformulated (as demonstrated in Appendix VIII):

$$\Delta P_e = \tilde{K}_S\Delta\delta + \tilde{K}_D\Delta\omega + (\tilde{K}_{SS}\Delta\delta + \tilde{K}_{DD}\Delta\omega) \frac{\Delta F_2(\tilde{\lambda}_p)}{K_2}, \quad (23)$$

with:

$$\begin{aligned} \tilde{K}_{SS} &= \tilde{K}_S + \frac{l_{12}}{l_{1d} + l_2} \tilde{K}_{S,AVR} + l_1 - K_1; \\ \tilde{K}_{DD} &= \tilde{K}_D + \frac{l_{12}}{l_{1d} + l_2} \tilde{K}_{D,AVR}, \end{aligned} \quad (24)$$

where $\tilde{K}_{S,AVR}$ and $\tilde{K}_{D,AVR}$ represent the contributions of $\tilde{\Gamma}_{avr}(\tilde{\lambda}_p)$ to the synchronizing and damping torque coefficients [20], respectively.

Now, let the supplementary HVDC controller $F(s)$ be designed as:

$$F(s) = -s \cdot K_{DC}, \quad (25)$$

where K_{DC} is the gain of the HVDC controller, and output is proportional to a local frequency. For the purpose of supporting frequency stability, a simple control of the HVDC active power injection proportional to frequency deviation is often considered as a safe and robust choice. Such control improves the closed-loop stability margin of the transfer function that connects the system frequency with the total active power balance [6]–[8].

As given in (53) of Appendix A, the control from (25) directly affects the function $W(s)$. By accounting for the HVDC contribution, at the mode of interest $\tilde{\lambda}_p = s = \sigma_p + j\omega_p$, $W(s)$ may be represented as:

$$W(s) = \frac{sK_{DC}}{l_{12} + sK_{DC}}|_{s=\tilde{\lambda}_p} = \frac{K_{DC}(\sigma_p + j\omega_p)}{l_{12} + K_{DC}(\sigma_p + j\omega_p)}. \quad (26)$$

For further derivations, it is convenient to distinguish between the real (W_R) and imaginary (W_I) parts of $W(s)$:

$$W_R = K_{DC} \frac{\sigma_p l_{12} + (\sigma_p^2 + \omega_p^2) K_{DC}}{(l_{12} + K_{DC}\sigma_p)^2 + \omega_p^2 K_{DC}^2}; \quad (27)$$

$$W_I = K_{DC} \frac{\omega_p l_{12}}{(l_{12} + K_{DC}\sigma_p)^2 + \omega_p^2 K_{DC}^2}. \quad (28)$$

By the virtue of (20) and (57), the changes in synchronizing ΔK_S and damping ΔK_D coefficients can be expressed with respect to the real and imaginary parts of $W(s)$:

$$\Delta K_S = \frac{l_1}{l_{12}} \left[\tilde{K}_{SS} \left(W_R - \frac{\sigma_p}{\omega_p} W_I \right) - \tilde{K}_{DD} \frac{\lambda_p^2}{\omega_p} W_I \right]; \quad (29)$$

$$\Delta K_D = \frac{l_1}{l_{12}} \left[\tilde{K}_{DD} \left(W_R + \frac{\sigma_p}{\omega_p} W_I \right) + \tilde{K}_{SS} \frac{1}{\omega_p} W_I \right], \quad (30)$$

from which the incorporation of (27)–(28) finally yields:

$$\Delta K_S = \frac{l_1 K_{DC} \lambda_p^2 [\tilde{K}_{SS} K_{DC} - l_{12} \tilde{K}_{DD}]}{l_{12} [(l_{12} + \sigma_p K_{DC})^2 + (\omega_p K_{DC})^2]}; \quad (31)$$

$$\Delta K_D = \frac{l_1 K_{DC} [\tilde{K}_{DD} (\lambda_p^2 K_{DC} + 2\sigma_p l_{12}) + l_{12} \tilde{K}_{SS}]}{l_{12} [(l_{12} + \sigma_p K_{DC})^2 + (\omega_p K_{DC})^2]}. \quad (32)$$

Hereby, the explicit analytical relationships between the gain K_{DC} of HVDC supplementary power control (control proportional to bus frequency) and change in synchronizing and damping coefficients $\Delta K_{S/D}$ are derived.

IV. THE ANALYSIS OF DERIVED EXPRESSIONS

The derived changes in synchronising and damping coefficients ($\Delta K_{S/D}$) from (31)–(32) are functions of both the mode of interest $\bar{\lambda}_p$ and the synchronizing/damping (\tilde{K}_S/\tilde{K}_D) coefficients from “no-HVDC-control-case”. An increase of gain K_{DC} to a non-zero value causes the “HVDC gain-mode” interactions, i.e. ΔK_S and ΔK_D resulting from the HVDC control change simultaneously with $\Delta \bar{\lambda}_p$. Since the high dimensionality of the problem and its very nature do not allow to solve for the new characteristic polynomial of the system state matrix, it is not possible to analytically determine a new $\bar{\lambda}_p + \Delta \bar{\lambda}_p$ in a general case. However, this issue can be addressed numerically by calculating $\bar{\lambda}_p + \Delta \bar{\lambda}_p$ from the equivalent state matrix which then enables the identification of $\Delta K_{S/D}$.

Some existing works have been addressing the similar problem for the case of other power system components (Static Var Compensator, AVRs and PSSs). However, in these studies, either the analytical expression for $\Delta K_{S/D}$ was not derived [24] or the effect on $\Delta K_{S/D}$ was assessed through some extensive sensitivity analysis [25], [26]. In [23], an analytical expression was determined to show the PSS contribution to $\Delta K_{S/D}$. That work used the assumption that is equivalent to the one from (22) of this paper. Additionally, a possible solution to the analytical problem was proposed in [27] where $\Delta K_{S/D}$ were calculated iteratively. Nevertheless, both of these analyses have focused on the effect of AVR and PSS only. This paper further investigates the properties of developed expressions and provides an insight into SSS phenomena that are related to specific HVDC control gains.

A. Mathematical Properties of ΔK_S and ΔK_D

By taking into account the aforementioned results and observations, the rest of this paper analyses the general behavior of $\Delta K_{S/D}$ functions with respect to the HVDC gain K_{DC} . Here, it was considered that $\bar{\lambda}_p$ is not changing as K_{DC} increases (as for (22)). Since poorly damped modes are of interest, it can also be assumed that $\sigma_p^2 \ll \omega_p^2$ and $\sigma_p \tilde{K}_{DD} \approx 0$.

(i) Now, let $K_{DC} \approx 0$ be a small positive value. Then the following expressions can be derived:

$$\Delta K_S = \frac{-l_1 K_{DC} \lambda_p^2 \tilde{K}_{DD}}{l_{12}^2}; \Delta K_D = \frac{l_1 K_{DC} \tilde{K}_{SS}}{l_{12}^2}. \quad (33)$$

By the virtue of (58) from Appendix B, $\Delta K_D > 0$ holds always and if $\tilde{K}_{DD} < 0$ then also $\Delta K_S > 0$. Equation (58) assumes that AVR and PSS have an overall positive impact on K_S and that respective angles (δ, θ) are in a reasonable range.

(ii) For $\tilde{K}_{DD} > 0$, it can be noted that ΔK_S is non-negative as long as it is satisfied that:

$$\tilde{K}_{SS} K_{DC} - l_{12} \tilde{K}_{DD} \geq 0 \Leftrightarrow K_{DC} \geq \frac{l_{12} \tilde{K}_{DD}}{\tilde{K}_{SS}}. \quad (34)$$

Although a theoretical condition for $\Delta K_S < 0$ exists, the typical values of the given parameters imply that this effect is negligible, as it will be afterwards shown in the case study.

(iii) At the maximum value of ΔK_D , it is valid that:

$$\frac{d(\Delta K_D)}{dK_{DC}} = 0. \quad (35)$$

The solution of (35) yields the expression for the HVDC controller gain for the maximal damping coefficient as:

$$K_{DC}^{opt} = l_{12} \left(\frac{\tilde{K}_{DD}}{\tilde{K}_{SS}} + \sqrt{\left(\frac{\tilde{K}_{DD}}{\tilde{K}_{SS}} \right)^2 + \frac{1}{\omega_p^2}} \right). \quad (36)$$

It is important to outline that the maximum value indeed exists, and that it can be referred to as the maximum/optimum value for a given operating condition. By taking typical operating conditions and parameters, it can be shown that this value is quite high—sufficiently high to ensure the SSS of the system.

(iv) For large gains (dominant K_{DC}^2 terms), it holds that:

$$\Delta K_S = \frac{l_1}{l_{12}} \tilde{K}_{SS}; \Delta K_D = \frac{l_1}{l_{12}} \tilde{K}_{DD}, \quad (37)$$

from where it also becomes clear that ΔK_S remains positive and ΔK_D is having the same sign as \tilde{K}_{DD} . Equation (37) implies that K_D decreases ($\Delta K_D < 0$) for $\tilde{K}_{DD} < 0$ and very large HVDC gains. The damping for the case of an “infinite” HVDC gain is, in fact, equivalent to the damping of an open loop zero which is independent of HVDC controller type.

B. Comparison of Analytical and Simulation Results

The subsequent analysis is provided for the Single-Machine Infinite-Bus (SMIB) system from Fig. 1 which is modelled in Solvina’s Simpow software. The AVR and PSS are tuned by the means of the “residue” method [4] to improve the system transient response and SSS. The injection of the HVDC system is modeled via back-to-back connection to another infinite bus. The study examines six distinct cases, involving:

- 1) three different HVDC system locations:
 - **Location 1:** $x_1 = 0.2$ (pu) and $x_2 = 0.2$ (pu),
 - **Location 2:** $x_1 = 0.3$ (pu) and $x_2 = 0.1$ (pu),
 - **Location 3:** $x_1 = 0.1$ (pu) and $x_2 = 0.3$ (pu) and
- 2) two levels of PSS gain: $K_{PSS_1} = 1$ and $K_{PSS_2} = 10$.

As an example, the changes in synchronizing and damping coefficients for “**Location 1**/ K_{PSS_1} ” and “**Location 3**/ K_{PSS_2} ” cases are visualised in Fig. 3. The active power provided by the generator is 100 (MW) (nominal). The generator data, PSS and AVR settings are listed within Table I of Appendix C. With respect to the size of the system and the HVDC control purpose, $K_{DC} = 500$ (pu) = 1000 (MW/Hz) is found to be the maximum reasonable gain value to be used for investigating the presented control. Higher gain values could cause the instability during nonlinear transient response as well as numerical issues in simulations.

The case depicted in Fig. 3 includes:

- 1) The results obtained analytically by (31) and (32);
- 2) The numerical results provided by Simpow software;
- 3) Results that originate from the exact expressions (14)–(16) for the AVR and PSS contributions. These equations were derived analytically in Section II, but to be solved for

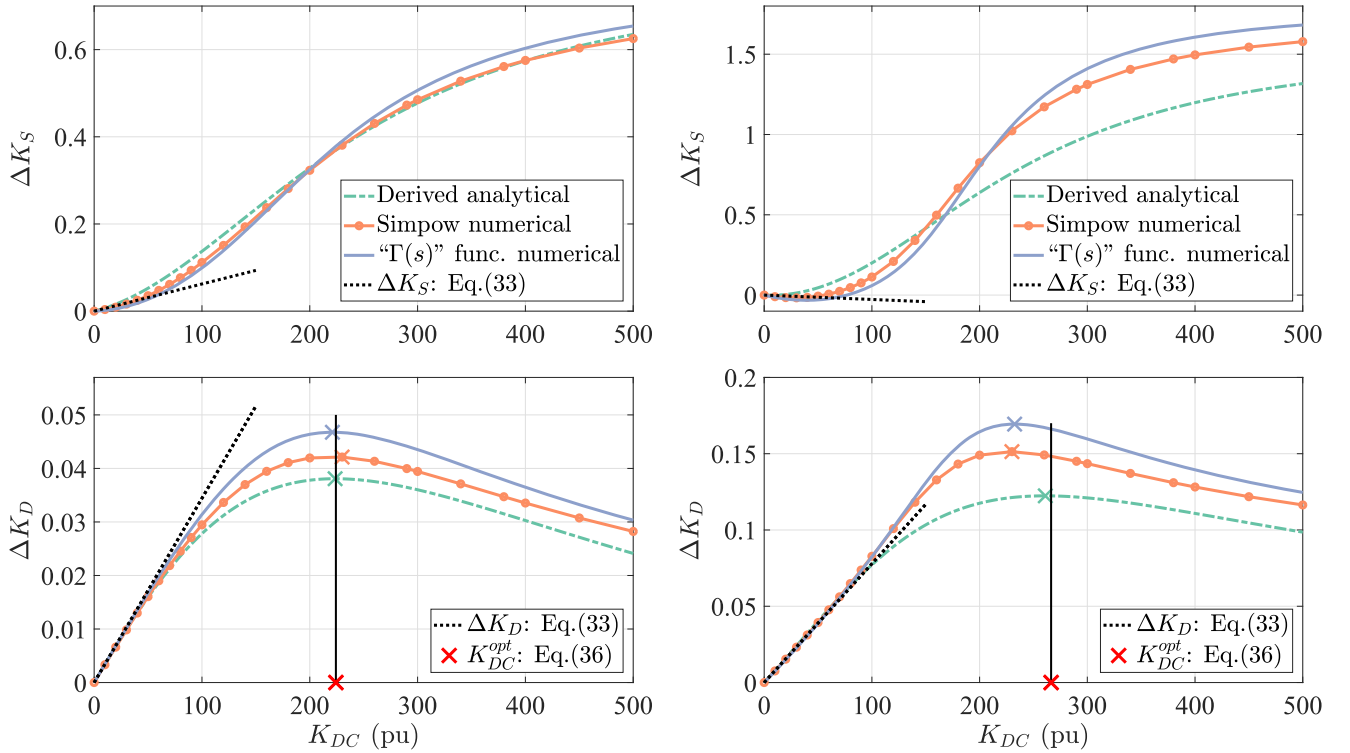


Fig. 3. The change of $K_{S/D}$ coefficients with respect to K_{DC} for: (a) **Location 1**/ K_{PSS_1} with initial mode $\bar{\lambda}_p = 0.1066 + j2\pi \cdot 1.2217$ (left figures) and (b) **Location 3**/ K_{PSS_2} with initial mode $\bar{\lambda}_p = -1.2269 + j2\pi \cdot 1.1787$ (right figures).

respective coefficients a numerical approach from Matlab R2017b had to be used;

- 4) The approximate ΔK_S and ΔK_D from (33) that have been defined for a small, positive K_{DC} value.

Apparently, as can be seen from Fig. 3, the results from the analytical approach follow the results obtained by the software. The (small) mismatch between the analytically and numerically obtained results comes from unmodeled HVDC back-to-back dynamics and stated assumptions. This even holds for the approximated expressions from (33) that were derived for smaller variations of K_{DC} . The graphical representation of these expressions from Fig. 3 is exactly matching the three curves for the “lower” values of the HVDC gain, acting as a tangent that defines the initial slope of the curves.

Figure 3 also demonstrates that there indeed exists a maximum value ΔK_D^{max} for K_{DC}^{opt} starting from which the damping coefficient is decreasing. Additionally, the derived value of K_{DC}^{opt} from (36) (given by a red marker) appears not to deviate much from K_{DC} obtained for ΔK_D^{max} by the three methods, which is an encouraging result. One may also notice that an HVDC control placed closer to the generator (as in the right figures) has a higher impact on the both torque coefficients, as expected. The upper-right graph from Fig. 3 demonstrates that a high PSS gain causes $\bar{K}_{DD} > 0$ which further results in slight decrease of K_S for small HVDC gains (the opposite case applies to the upper-left graph). This observation is in line with (33).

Even though there is a difference between the analytical and numerical results, this study does not focus on substituting the numerical approach. It rather aims to explain the nature and

properties of an “HVDC-generator” interaction. In this sense, the authors believe that it was essential to first prove the existence of an optimal HVDC gain value (K_{DC}^{opt}) and then detect both the range of its values and its dependency to system and control parameters, as shown in (36). If the purpose of a study of similar type is to obtain as precise numerical results as possible, then the authors recommend the usage of appropriate software programs instead.

To quantify, the deviations between analytically derived $\Delta K_S^{Der.An.}$ and $\Delta K_D^{Der.An.}$ (from (31) and (32)) and the ones calculated numerically by Simpow software ($\Delta K_S^{Sim.}$ and $\Delta K_D^{Sim.}$) are found in percentage as:

$$\begin{aligned} \Delta K_S^{dev} &= \left| \frac{\Delta K_S^{Sim.} - \Delta K_S^{Der.An.}}{K_S^{Sim.}} \right| \cdot 100\%; \\ \Delta K_D^{dev} &= \left| \frac{\Delta K_D^{Sim.} - \Delta K_D^{Der.An.}}{\Delta K_D^{Sim.}} \right| \cdot 100\%, \end{aligned} \quad (38)$$

where the Simpow results ($K_S^{Sim.}$ and $\Delta K_D^{Sim.}$, respectively) serve as the reference. For a set of K_{DC} values, the maximum, minimum and mean values for all the six tested cases are summarized in Fig. 4.

Although the mean ΔK_D^{dev} increases together with K_{DC} , derived $\Delta K_D^{Der.An.}$ is still able to capture a general behavior of K_D under the influence of the HVDC control. The similar tendency was observed for K_S . It is reasonable to expect an increase in ΔK_D^{dev} since the stated assumptions are more affected in the presence of very large HVDC gains, which some of the tested ones certainly are.

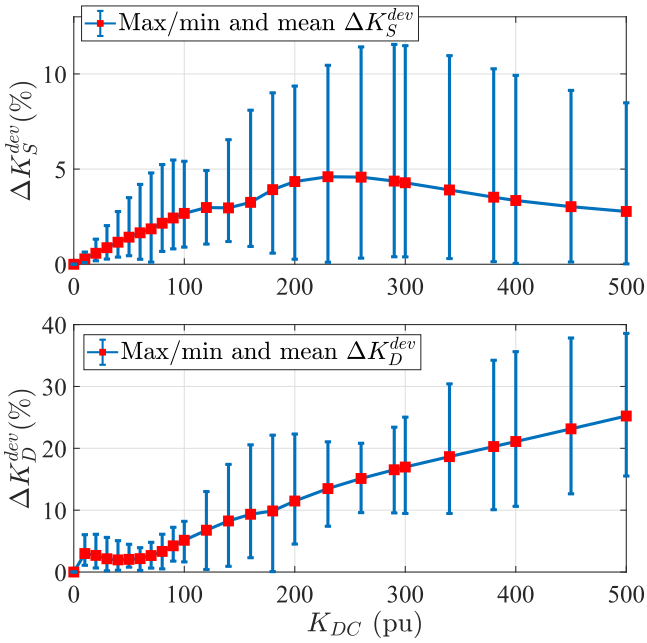


Fig. 4. Max/min and mean ΔK_S^{dev} and ΔK_D^{dev} values for the six test cases.

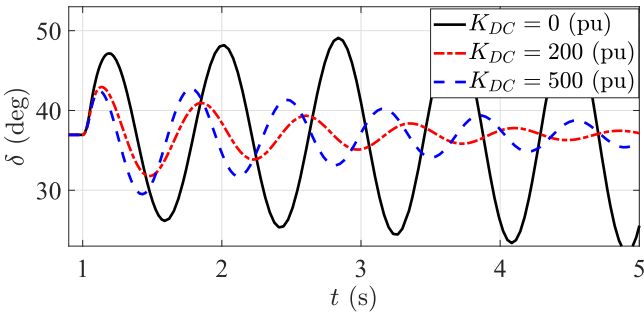


Fig. 5. Simulation result of the fault response for three cases of HVDC gain.

Now, in the same system, the effect of the applied HVDC control is tested through a non-linear time domain simulation of a three-phase short circuit on the line between PCC and the infinite bus. By clearing the fault without changes in configuration, the time response for three different values of K_{DC} is given in Fig. 5 for case “**Location 1**/ K_{PSS1} ”.

In this figure, one may notice that the rotor angle oscillations of the generator become more damped with the increase of K_{DC} from 0 to 200 (pu). However, a “too large” HVDC gain (i.e. $K_{DC} = 500$ (pu) $>$ K_{DC}^{opt}) causes the oscillations to become less damped. This implies that, beside affecting SSS, an inadequate HVDC gain can as well trigger an unwanted non-linear response of the system to large disturbances. Hence, this issue should be systematically addressed.

In a multi-machine power system, all the modes are of interest and all may be affected to some extent by a supplementary HVDC control. Typically, the electromechanical modes have the least damping and therefore, it is of interest to assess the associated interactions—especially those occurring between the generators and HVDC links that are “electrically” closer. Hence, it is reasonable to argue that a similar multi-machine

phenomenon can be correlated to the presented SMIB system study and consequently, to the results of the provided analysis that focused on the generic conclusions regarding the nature of the most prominent interaction.

In order to get a better insight into the effects of a supplementary HVDC control, the further analysis is to focus on occurrences in a multi-machine system. The main goals will be to identify the modes that are prone to being affected by the controller and to provide quantitative results of this interaction that are comparable with the outcomes of the SMIB study.

V. DISCUSSION

A. Frequency and SSS HVDC Support

Having the full or high observability of the system dynamics increases the chances for a significant improvement of the controller efficiency. In those cases, different and more sophisticated tuning methods can be applied. Preferably, a tuning that both covers the whole frequency range and is also resilient to the uncertainties in system operation and parameters is desired. Furthermore, the controller performance depends on input/output signals, controller structure and its possibility to adapt the settings according to the changes in the system.

Some of the previous linear studies assessed the sophisticated (H_∞ and H_2) controllers to cover for the frequencies in the range of electromechanical oscillations [19], [28], [29]. Those methods establish the appropriate weight functions and input signals in order to achieve desired closed-loop transfer functions. A typical, however, more conservative solution, is to tune the controller’s phase compensation (with restrictive dynamics order) to target the desired frequencies [30]. Still, the employment of PID or more simple—droop (proportional) controllers could be a beneficial solution, especially with having the correct (remote) input signals available [9]–[12], [15]–[17]. Yet, the observability of realistic systems and their communication infrastructure could be insufficient for such advanced tuning. Therefore, a reduction in the controller design and the restriction to use reliable local measurements might be imposed.

The controller investigated in the article is not primarily designed to provide Power Oscillation Damping (POD) control service. The main purpose of this controller is frequency regulation, while the side-effects of its application are thoroughly investigated in the paper. The practical implementation of frequency control requires specific assessment which differs from the procedure used to tune POD controllers in the sense that frequency controllers do not require a high observability (of different system states) since they are mainly designed to improve the system frequency response. However, in low inertia systems, HVDC frequency control gains might have to be large in order to support the system response. Such action would then also have a significant impact on the electromechanical modes of the generators which are “electrically” close to the HVDC interconnections that provide frequency control.

B. The Impact of Governor/Turbine Dynamics

It is furthermore important to highlight that the influence of the HVDC supplementary control on the modes behavior is

assessed for the least damped mode in the system (which is typically an electromechanical mode). Therefore, this mode can be considered as a good representation of the system dynamics. The frequency of this mode is usually between 0.1 and 3 Hz. Considering the timescale of the electromechanical dynamics, the presence of turbines should not significantly impact the behavior of the assessed mode. The turbine constants are usually in the range of several seconds, depending on the generator size and type, so no major interaction is expected.

It should be outlined that, strictly speaking, any additional controls/dynamics affect the positions of the modes in the complex plot. To check if these dynamics pose a significant impact on the nature of the observed interaction, let us introduce the turbine and governor dynamics $\Gamma_M(s)$. One may notice that $\Gamma_{avr}(s)$ and $\Gamma_{pss}(s)$ are dependent on the HVDC control while the governor/turbine dynamics are not.

The linearized swing dynamics, without the inclusion of an HVDC supplementary control, can be described as:

$$-Ms\Delta\omega = \Delta P_e(s) - \Delta P_m(s), \quad (39)$$

where the electrical and mechanical power contributions are:

$$\begin{aligned} \Delta P_e(s) &= \left(K_1 + \tilde{\Gamma}_{avr}(s) + s\tilde{\Gamma}_{pss}(s) \right) \Delta\delta; \\ \Delta P_m(s) &= \Gamma_M(s)\Delta\omega, \end{aligned} \quad (40)$$

respectively. By focusing on the properties of the most critical, electromechanical mode ($s = \bar{\lambda}_p$), the system dynamics may be described in terms of equivalent synchronizing and damping components that can be obtained from their corresponding electrical and mechanical power contributions:

$$\{-Ms\Delta\omega\}_{s=\bar{\lambda}_p} = \Delta P_e(s = \bar{\lambda}_p) - \Delta P_m(s = \bar{\lambda}_p), \quad (41)$$

from which, after some mathematical manipulations, it yields:

$$\begin{aligned} -M(\sigma_p + j\omega_p)\Delta\omega &= (\tilde{K}_S\Delta\delta + \tilde{K}_D\Delta\omega) \\ &\quad + (\tilde{K}_{Sm}\Delta\delta + \tilde{K}_{Dm}\Delta\omega) \\ \Leftrightarrow -M(\sigma_p + j\omega_p)\Delta\omega &= \tilde{K}_{Seq}\Delta\delta + \tilde{K}_{Deq}\Delta\omega. \end{aligned} \quad (42)$$

With the inclusion of the HVDC supplementary control, the modifications are to be made only in $\Delta P_e(s)$ (and not in $\Delta P_m(s)$), as it has been previously derived. It also holds that $\tilde{\Gamma}_{avr}(s) \neq \Gamma_{avr}(s)$ and $\tilde{\Gamma}_{pss}(s) \neq \Gamma_{pss}(s)$ while $\Gamma_M(s)$ remains the same despite the HVDC inclusion.

The changes in synchronizing (ΔK_S) and damping (ΔK_D) components caused by the inclusion of the HVDC supplementary power control are here studied for a typical steam- and hydro- governor/turbine design, taken from [4]. The generator data, PSS and AVR settings (available in Appendix C) from SubSection IV-B are retained. The numerical analysis has been carried out for **Location 3** ($x_1 = 0.1$ (pu) and $x_2 = 0.3$ (pu)) and K_{PSS1} . The results were obtained by employing:

- 1) The derived analytical expressions (31) and (32);
- 2) A numerical tool (Matlab software) where the poles of the system were calculated from the transfer function:

$$G(s) = \frac{1}{Ms^2 + F_1(s) + \Gamma_{avr}(s) + s\Gamma_{pss}(s) - \Gamma_M(s)}, \quad (43)$$

and the coefficients were identified by using:

$$K_S = \lambda_p^2 M; \quad K_D = -2\sigma_p M. \quad (44)$$

From the results summarized in Fig. 6, it can be observed that there is no major impact of the included turbine/governor dynamics on the interaction of interest. This holds regardless of: (i) the position of the HVDC PCC or (ii) the PSS gain.

VI. CONCLUSION

Currently, there is a progressive tendency to address stability challenges in modern AC systems through the employment of fast and flexible grid elements, such as HVDC interconnections. This paper has investigated some interesting stability side-effects of a supplementary (proportional) HVDC power control that is primarily intended for the frequency support.

For this purpose, the paper has employed a linear analysis to investigate how an HVDC control may affect electromechanical dynamics. An extensive analysis was carried out for a generic system to understand the underlying mechanism of undesired decrease in system damping due to a wrong/too-high choice of the HVDC controller gain. The presented study overcomes the challenging (direct) incorporation of the local signal as an input to the HVDC control while also including AVR/PSS dynamics. In that sense, the paper derived the change in torque coefficients as the explicit functions of HVDC gain K_{DC} . The established functional relationships were then compared (and found to be in line) with the results of numerical analysis in SMIB case study.

The given approach introduces a plausibility of various SSS scenarios provided that the applied HVDC control, AVR and PSS satisfy specific conditions (meaning that these components need to be considered jointly in stability assessment). As a final conclusion, the paper has shown that the examined type of HVDC controller can (i) improve the frequency, SSS and transient stability when being in its ‘‘range of positive impact’’ ($K_{DC} < K_{DC}^{opt}$) or (ii) worsen electromechanical response if that is not the case. The general approach to control design makes the study applicable to other controllers. The main research lines of the future work involve a further analysis of the conditions for the negative influence of the presented control as well as the identification of stability measures for mitigation of such conditions.

APPENDIX A

The content of this Appendix is intended for supporting the mathematical definitions and derivations of Section II. There, the electrical powers from (3a)–(3b) are given as:

$$P_1 = \frac{E'_q U}{x_1 + x'_d} \sin(\delta - \theta) = P_e; \quad P_2 = -\frac{UU_N}{x_2} \sin\theta; \quad (A.45a)$$

$$Q_1 = \frac{U^2 - E'_q U \cos(\theta - \delta)}{x_1 + x'_d}; \quad Q_2 = \frac{U^2 - UU_N \cos\theta}{x_2}, \quad (A.45b)$$

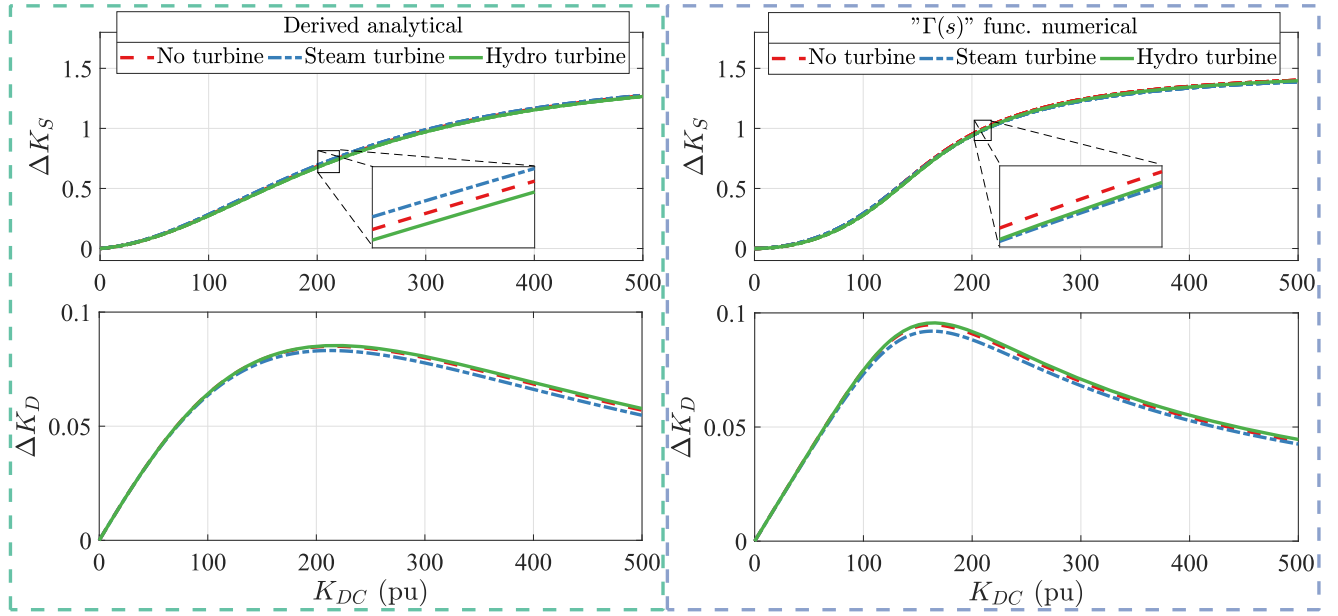


Fig. 6. The comparison of the case study results for different: (i) turbine types and (ii) approaches for the calculation of the changes in ΔK_S and ΔK_D that occurred with the inclusion of the HVDC supplementary control.

for which it holds the steady-state (operating point) equality:

$$\begin{aligned} P_{10} &= -P_{20} = \frac{E'_{q0}U_0}{x_1 + x'_d} \sin(\delta_0 - \theta_0) = P_{e0}; \\ Q_{10} &= -Q_{20} = \frac{U_0^2 - E'_{q0}U_0 \cos(\theta_0 - \delta_0)}{x_1 + x'_d}. \end{aligned} \quad (\text{A.46})$$

To simplify the linearized expressions of Section II, it is convenient to define the following entities:

$$\begin{aligned} l_1 &= \frac{E'_{q0}U_0}{x_1 + x'_d} \cos(\delta_0 - \theta_0); \quad l_2 = \frac{U_0U_N}{x_2} \cos\theta_0; \\ l_d &= \frac{E'_{q0}U_{t0}}{x'_d} \cos(\delta_0 - \theta_{t0}); \quad l_{1d} = \frac{U_{t0}U_0}{x_1} \cos(\theta_{t0} - \theta_0). \end{aligned} \quad (\text{A.47})$$

Then, by taking into account the contribution of the HVDC control, the linearized dynamics of $\Delta E'_q$ is represented as:

$$\begin{aligned} T'_{do}s\Delta E'_q &= \frac{x_d - x'_d}{x_1 + x'_d} \cos(\delta_0 - \theta_0)\Delta U - \frac{x_1 + x_d}{x_1 + x'_d} \Delta E'_q \\ &+ \Delta E_f - \frac{x_d - x'_d}{x_1 + x'_d} U_0 \sin(\delta_0 - \theta_0)(\Delta\delta - \Delta\theta) \\ &= \Delta E_f - \left[\frac{(x_d - x'_d)P_{e0}}{E'_{q0}} \left(\frac{l_2 - F(s)}{l_{12} - F(s)} + \frac{l_1}{l_{12}} \right) \right] \Delta\delta \\ &+ \left[\frac{(x_d - x'_d)}{E'_{q0}} \left(\frac{l_1^2}{l_{12}} + \frac{P_{e0}^2}{l_{12} - F(s)} \right) - \frac{x_1 + x_d}{x_1 + x'_d} \right] \Delta E_q, \end{aligned} \quad (\text{A.48})$$

from which the corresponding functions (that figure in (14)) can be expressed in a convenient form:

$$\begin{aligned} F_4(s) &= \frac{(x_d - x'_d)P_{e0}}{E'_{q0}} \left(\frac{l_2 - F(s)}{l_{12} - F(s)} + \frac{l_1}{l_{12}} \right) \\ \frac{1}{F_3(s)} &= -\frac{(x_d - x'_d)}{E'_{q0}} \left(\frac{l_1^2}{l_{12}} + \frac{P_{e0}^2}{l_{12} - F(s)} \right) + \frac{x_1 + x_d}{x_1 + x'_d}. \end{aligned} \quad (\text{A.49})$$

Finally, by linearizing the dynamics of excitation voltage E_f :

$$T_e s \Delta E_f = -\Delta E_f - K_A \Delta U_t, \quad (\text{A.50})$$

it becomes clear that the relationship between ΔU_t and state variables needs to be determined. After several algebraic manipulations (similarly as in ΔU case), from the reactive power balance for the terminal bus one may easily obtain:

$$\begin{aligned} \Delta U_t &= \frac{U_{t0}}{l_{1d} + l_d} \left[-P_{e0} \left(\frac{l_{1d}}{l_{12}} + \frac{l_2 - F(s)}{l_{12} - F(s)} \right) \Delta\delta \right. \\ &\left. + \frac{1}{E'_{q0}} \left(\frac{P_{e0}^2}{l_{12} - F(s)} + l_d + \frac{l_1 l_{1d}}{l_{12}} \right) \Delta E'_q \right], \end{aligned} \quad (\text{A.51})$$

which then yields the remaining $F_i(s)$ functions from (14):

$$\begin{aligned} F_5(s) &= -\frac{U_{t0}}{l_{1d} + l_d} P_{e0} \left(\frac{l_{1d}}{l_{12}} + \frac{l_2 - F(s)}{l_{12} - F(s)} \right); \\ F_6(s) &= \frac{U_{t0}}{(l_{1d} + l_d)E'_{q0}} \left(\frac{P_{e0}^2}{l_{12} - F(s)} + l_d + \frac{l_1 l_{1d}}{l_{12}} \right). \end{aligned} \quad (\text{A.52})$$

Once having all $F_i(s)$ functions, it is straightforward to obtain the HVDC control contributions $\Delta F_i(s)$ from (15) as:

$$\begin{aligned}\Delta F_1(s) &= \frac{l_1^2}{l_{12}} W(s); \Delta F_4(s) = \frac{(x_d - x'_d) P_{e0} l_1 W(s)}{E'_{q0} l_{12}}; \\ \Delta F_2(s) &= \frac{P_{e0} l_1}{E'_{q0} l_{12}} W(s); \Delta F_5(s) = \frac{-U_{t0} P_{e0} l_1 W(s)}{(l_1 d + l_d) l_{12}}; \\ \Delta F_3(s) &= \frac{(x_d - x'_d) P_{e0}^2 W(s)}{E'_{q0} l_{12}}; \Delta F_6(s) = \frac{-U_{t0} P_{e0}^2 W(s)}{(l_1 d + l_d) l_{12} E'_{q0}}; \\ W(s) &= \frac{-F(s)}{l_{12} - F(s)}.\end{aligned}\tag{A.53}$$

APPENDIX B

This appended section follows the derivations of the synchronizing and damping torque coefficients from Section III. As the first step, the change in active generator power when an HVDC supplementary controller is installed may be easily obtained by combining (16) and (17):

$$\begin{aligned}\Delta P_e &= (\Gamma_{avr}(s) + F_1(s)) \Delta \delta + \Gamma_{pss}(s) \Delta \omega \\ &= (\tilde{\Gamma}_{avr}(s) + K_1) \Delta \delta + \tilde{\Gamma}_{pss}(s) \Delta \omega \\ &+ \left[\tilde{\Gamma}_{avr}(s) \left(\frac{\Delta F_2(s)}{K_2} + \frac{\Delta F_5(s)}{K_5} \right) + \Delta F_1(s) \right] \Delta \delta \\ &+ \underbrace{\tilde{\Gamma}_{avr}(s) \frac{\Delta F_2(s) \Delta F_5(s)}{K_2 K_5} \Delta \delta + \tilde{\Gamma}_{pss}(s) \frac{\Delta F_2(s)}{K_2} \Delta \omega}_{\approx 0}.\end{aligned}\tag{B.54}$$

By accounting for (22) and (53), it can be written:

$$\begin{aligned}\Delta P_e &= (\tilde{K}_S \Delta \delta + \tilde{K}_D \Delta \omega) \left(1 + \frac{\Delta F_2(\bar{\lambda}_p)}{K_2} \right) \\ &+ \left(\frac{l_{12}}{l_1 d + l_2} \tilde{K}_{S,AVR} - K_1 + l_1 \right) \frac{\Delta F_2(\bar{\lambda}_p)}{K_2} \Delta \delta \\ &+ \frac{l_{12}}{l_1 d + l_2} \tilde{K}_{D,AVR} \frac{\Delta F_2(\bar{\lambda}_p)}{K_2} \Delta \omega \\ &= (\tilde{K}_S \Delta \delta + \tilde{K}_D \Delta \omega) + (\tilde{K}_{SS} \Delta \delta + \tilde{K}_{DD} \Delta \omega) \frac{\Delta F_2(\bar{\lambda}_p)}{K_2},\end{aligned}\tag{B.55}$$

where the coefficients from the “no-HVDC-case” are:

$$\begin{aligned}\tilde{K}_S &= \tilde{K}_{S,AVR} + K_1 + \tilde{K}_{S,PSS}; \\ \tilde{K}_D &= \tilde{K}_{D,AVR} + \tilde{K}_{D,PSS},\end{aligned}\tag{B.56}$$

which then implies:

$$\Delta K_S \Delta \delta + \Delta K_D \Delta \omega = [\tilde{K}_{SS} \Delta \delta + \tilde{K}_{DD} \Delta \omega] \frac{l_1}{l_{12}} W(\bar{\lambda}_p).\tag{B.57}$$

In this paper, it was assumed that the following is valid:

$$\tilde{K}_{S,AVR} + l_1 > |\tilde{K}_{S,PSS}| \Rightarrow \tilde{K}_{SS} > 0.\tag{B.58}$$

APPENDIX C

The system parameters related to generator data, AVR and

TABLE I
GENERATOR DATA, AVR AND PSS SETTINGS

Generator							
S_n	U_n	f_n	H	D	x_d	x'_d	x_t
(MVA)	(kV)	(Hz)	(s)	(pu)	(pu)	(pu)	(pu)
100	230	50	4	0	1	0.15	0.1
AVR				PSS			
K_A	T_e	ω_n	T_W	T_1	T_2	n_f	K_{pss}
(pu)	(s)	(rad/s)	(s)	(s)	(s)	(#)	(pu)
150	0.01	$2\pi f_n$	10	0.2189	0.0775	1	-1/-10

PSS settings that were used in the case studies from SubSection IV-B and Section V are listed in the sequel within Table I.

REFERENCES

- [1] R. L. Evans, *Fueling Our Future: An Introduction to Sustainable Energy*. Cambridge, U.K.: Cambridge Univ. Press, 2007.
- [2] P. D. Lund *et al.*, *Advances in Energy Systems: The Large-Scale Renewable Energy Integration Challenge*. Hoboken, NJ, USA: John Wiley & Sons, 2019.
- [3] M. Kuivaniemi, N. Modig, and R. Eriksson, “FCR-D design of requirements,” ENTSO-E Rep., Jul. 2017.
- [4] P. Kundur, *Power System Stability and Control*. New York, NY, USA: McGraw-Hill, 1994.
- [5] M. Khenar *et al.*, “A control strategy for a multi-terminal HVDC network integrating wind farms to the AC grid,” *Int. J. Elect. Power Energy Syst.*, vol. 89, pp. 146–155, Jul. 2017.
- [6] D. Obradović, M. Ghandhari, and R. Eriksson, “Assessment and design of frequency containment reserves with HVDC interconnections,” in *Proc. North Amer. Power Symp.*, Fargo, ND, USA, 2018, pp. 1–6.
- [7] D. Obradović *et al.*, “Assessment of HVDC frequency control methods in the nordic test system,” in *Proc. CIGRE Symp.*, Paris, France, Aug. 2020, pp. 1–10.
- [8] D. Obradović, “Coordinated frequency control between interconnected AC/DC systems,” Licentiate thesis, Division Elect. Power Energy Syst., KTH Royal, Inst. Technol., Stockholm, SE, Oct. 2020.
- [9] A. Vural, “Contribution of high voltage direct current transmission systems to inter-area oscillation damping: A review,” *Renewable Sustain. Energy Rev.*, vol. 57, pp. 892–915, Apr. 2016.
- [10] D. Jovcic, *High Voltage Direct Current Transmission: Converters, Systems and DC Grids*. Hoboken, NJ, USA: Wiley, 2019.
- [11] T. Smed and G. Andersson, “Utilising HVDC to damp power oscillations,” *IEEE Trans. Power Del.*, vol. 8, no. 2, pp. 620–627, Apr. 1993.
- [12] L. Harnerfors, N. Johansson, and L. Zhang, “Impact on interarea modes of fast HVDC primary frequency control,” *IEEE Trans. Power Syst.*, vol. 32, no. 2, pp. 1350–1358, Mar. 2017.
- [13] A. G. Endegnanew and K. Uhlen, “Global analysis of frequency stability and inertia in AC systems interconnected through an HVDC,” in *Proc. IEEE Int. Energy Conf.*, Leuven, Belgium, 2016, pp. 1–6.
- [14] R. Shah, R. Preece, and M. Barnes, “Dual-loop primary frequency regulation controller for VSC-HVDC system,” in *Proc. IEEE Manchester PowerTech*, Manchester, U.K., 2017, pp. 1–6.
- [15] O. Samuelsson and B. Eliasson, “Damping of electro-mechanical oscillations in a multimachine system by direct load control,” *IEEE Trans. Power Syst.*, vol. 12, no. 4, pp. 1604–1609, Nov. 1997.
- [16] O. Samuelsson, “Load modulation at two locations for damping of electro-mechanical oscillations in a multimachine system,” in *Proc. Power Eng. Soc. Summer Meeting* (Cat. No.00CH 37134), Seattle, WA, USA, 2000, pp. 1912–1917, vol. 3.
- [17] O. Samuelsson, “Load modulation for damping of electro-mechanical oscillations,” in *Proc. IEEE Power Eng. Soc. Winter Meeting* (Cat. No.01CH37194), Columbus, OH, USA, vol. 1, 2001, pp. 241–246.
- [18] J. L. Domínguez-García *et al.*, “Input-output signal selection for damping of power system oscillations using wind power plants,” *Int. J. Elec. Power*, vol. 58, pp. 75–84, Jun. 2014.

- [19] J. L. Domínguez-García, F. D. Bianchi, and O. Gomis-Bellmunt, "Control signal selection for damping oscillations with wind power plants based on fundamental limitations," *IEEE Trans. Power Syst.*, vol. 28, no. 4, pp. 4274–4281, Nov. 2013.
- [20] P. W. Sauer and M. A. Pai, *Power System Dynamics and Stability*, Upper Saddle River, NJ, USA: Prentice Hall, 1998.
- [21] F. P. Demello and C. Concordia, "Concepts of synchronous machine stability as affected by excitation control," *IEEE Trans. Power App. Syst.*, vol. PAS- 88, no. 4, pp. 316–329, Apr. 1969.
- [22] S. J. Mason, "Feedback theory—further properties of signal flow graphs," *Proc. IRE*, vol. 44, no. 7, pp. 920–926, Jul. 1956.
- [23] A. M. Yousef and M. K. El-Sherbiny, "Improvement of synchronizing and damping torque coefficients based LQR power system stabilizer," in *Proc. Int. Conf. Elect., Electron. Comput. Eng.*, Cairo, Egypt, 2004, pp. 753–758.
- [24] A. A. El-Emary, "Formula for the effect of a static VAR compensator on synchronising torque coefficient," *IEE Proc. Gen. Transmiss., Distrib.*, vol. 143, no. 6, pp. 582–586, Nov. 1994.
- [25] S. E. M. de Oliveira, "Synchronizing and damping torque coefficients and power system steady-state stability as affected by static VAR compensators," *IEEE Trans. Power Syst.*, vol. 9, no. 1, pp. 109–119, Feb. 1994.
- [26] S. E. M. de Oliveira, "Effect of excitation systems and of power system stabilisers on synchronous generator damping and synchronising torques," *IEE Proc. C. Gen. Transmiss., Distrib.*, vol. 136, no. 5, pp. 264–270, Sep. 1989.
- [27] W. K. Marshall and W. J. Smolinski, "Dynamic stability determination by synchronizing and damping torque analysis," *IEEE Trans. Power App. Syst.*, vol. PAS-92, no. 4, pp. 1239–1246, Jul. 1973.
- [28] J. S. Laverde and M. A. Ríos, "Damping electromechanical oscillations using supplementary controls at VSC-HVDC stations based on reduced low order models," *Control Eng. Pract.*, vol. 79, pp. 195–208, Oct. 2018.
- [29] J. Björk *et al.*, "Analysis of coordinated HVDC control for power oscillation damping," in *Proc. IEEE Electron. Power Grid (eGrid)*, Charleston, SC, USA, 2018, pp. 1–6.
- [30] R. Preece *et al.*, "Damping of inter-area oscillations using WAMS based supplementary controller installed at VSC based HVDC line," in *Proc. IEEE Trondheim PowerTech, Trondheim*, 2011, pp. 1–8.



Danilo Obradović (Student Member, IEEE) received the B.Sc. and M.Sc. degrees in electrical engineering from the Department of Power Systems, School of Electrical Engineering, University of Belgrade, Belgrade, Serbia, in 2016 and 2017, respectively, and the Licentiate degree in electrical engineering in 2020 from the Division of Electric Power and Energy Systems, KTH Royal Institute of Technology, Stockholm, Sweden, in 2020, where he is currently working toward the Ph.D. degree with the KTH Royal Institute of Technology. His research interests include

power system dynamics, stability and control, and HVDC systems.



Marina Oluic (Member, IEEE) received the B.Sc. and M.Sc. degrees in electrical engineering from the Faculty of Technical Sciences, University of Novi Sad, Serbia, in 2011 and 2012, respectively, and the joint Ph.D. degree in sustainable energy technologies and strategies from the Division of Electric Power and Energy Systems, KTH Royal Institute of Technology, Stockholm, Sweden, in 2019. The joint degree was issued by Comillas Pontifical University, Madrid, Spain, Delft University of Technology, Delft, The Netherlands, and KTH. She is currently a Post-doctoral Researcher with KTH. Her research interests include power system dynamics, stability, and control.



Robert Eriksson (Senior Member, IEEE) received the M.Sc. and Ph.D. degrees in electrical engineering from the KTH Royal Institute of Technology, Stockholm, Sweden, in 2005 and 2011, respectively. From 2013 to 2015, he held a position as an Associate Professor with Center for Electric Power and Energy, Technical University of Denmark - DTU, Kongens Lyngby, Denmark. He is currently with Swedish National Grid, Department of Power Systems. Since 2020, he has been an Adjunct Professor with the KTH Royal Institute of Technology. His current research interests include power system dynamics and stability, automatic control, HVDC systems, and dc grids.



Mehrdad Ghandhari (Senior Member, IEEE) received the M.Sc. and Ph.D. degrees in electrical engineering from the KTH Royal Institute of Technology (KTH), Stockholm, Sweden, in 1995 and 2000, respectively. He is currently a Full Professor with KTH. His research interests include power system dynamics, stability, and control, flexible ac transmission systems and HVDC systems, and linear and nonlinear control strategies.